Role of Dry Dynamics in the Maritime Continent Barrier Effect in the Madden Julian Oscillation

Paul E. Roundy

University at Albany
Albany, New York, United States
Corresponding Author, Paul E. Roundy, proundy@albany.edu

Abstract

Eastward-moving moist deep convection and atmospheric circulation signals associated with the tropical Madden Julian Oscillation (MJO) sometimes break down as they cross the Maritime Continent region, but other times the signal propagates across the region maintaining amplitude or regaining it over the West Pacific Basin. This paper assesses the hypothesis that upper tropospheric zonal diffluence of the background wind over the Maritime Continent causes much of this Maritime Continent barrier effect and its variation over time, through two mechanisms. 1. By slowing down the MJO as stronger than average background upper tropospheric zonal wind over the Indian Ocean advects the MJO circulation signal westward, slowing its eastward advance, and 2. through zonal advection of background wind by subseasonal zonal wind across a region of zonal diffluence of the background wind, which advects background wind of the opposite sign to the MJO wind. Advection of the opposite-signed background wind counteracts the MJO wind and reduces its associated upper tropospheric mass divergence, weakening the mechanisms of the upper tropospheric Kelvin wave component of the MJO circulation. Composites of MJO-associated zonal wind and outgoing longwave radiation signals diminish as they cross the Maritime Continent region when the region's background zonal winds are diffluent, and composites of data reconstructing the relevant advection terms reveal the direct action of the advection mechanisms.

Significance Statement: The Madden Julian oscillation (MJO) is the leading subseasonal variation of the tropical atmosphere. This project addresses how diffluence of the upper tropospheric background zonal wind can break down MJO events through advection of and by the background wind.

1. Introduction

The Madden Julian oscillation (MJO, Madden and Julian 1972) modulates the weather around the world as it moves eastward across the warm pool regions of the tropics at phase speeds typically less than 8 ms^{-1}. Although the associated atmospheric circulation signals move around the entire world, its average associated rainfall signals emerge strongest over the Indian Ocean, weaken near the Maritime Continent region, and grow again over the Western Pacific Ocean before finally weakening over the Central Pacific Ocean (Hendon and Salby 1994; Wheeler and Kiladis 1999; Roundy and Frank 2004). Although some MJO convective events continue across the Maritime Continent to the West Pacific region without much change of amplitude, the convective signals of other events almost completely break down before reaching the West Pacific basin (e.g., Zhang and Ling 2017, Demott et al. 2018, Ling et al. 2019, Kim et al. 2021, Zhou et al. 2022, and many others). This breakdown phenomenon is known as the Maritime Continent barrier effect. Numerical weather prediction and climate models tend to exhibit stronger barrier effects than observations, leading to a bias in these models with insufficient numbers of events getting through to the Pacific Basin (Abhik et al. 2023). This bias implies that the downstream outcomes associated with progression of the MJO across the Pacific region might also tend to occur less frequently in the models than in observations. The bias presents a forecast problem, as when the observed MJO ultimately does cross the Maritime Continent, a substantial and sometimes sudden change occurs in the middle latitude model forecast states.

Previous authors have analyzed clues pointing to several alternative explanations of the barrier effect (see Demott et al. 2018 and Kim et al. 2021 for summaries). To name a few, strong diurnal convection around the islands seems to interfere with subseasonal convection over the Maritime Continent (Ling et al. 2019; Ajayamohan et al. 2021). The islands also interfere with the organization of convection over water. Chen et al. (2020) showed that models that more strongly evolve the convection from land-dominated to ocean dominated during the regional active convective phase have Maritime Continent crossing rates closer to observations. The island region modifies the air sea sensible and latent heat fluxes relative to open ocean, and events that propagate through the Maritime Continent region have stronger and geographically broader air sea flux anomalies (Hudson and Maloney 2023), and broader, stronger moist anomalies (Barrett et al. 2021). Zhang and Han (2020) showed that events that cross the Maritime Continent tend occur less often when there is strong sea surface temperature contrast between the eastern Indian Ocean and the western Pacific Ocean. Demott et al. (2018) showed that many MJO events decline over the Maritime Continent when they intersect with westward-propagating dry anomalies, and that La Niña conditions favor the decline of MJO events. They also showed that many events that decline but that do not encounter dry westward-moving anomalies are associated with insufficient moistening over the southern Maritime Continent region. Other factors might include that winds modulated by the MJO ascending across topography can excite rainfall during the opposite MJO phase that on the large-scale favors convection, leading to atmospheric circulation responses counter to the concurrent state of the MJO.

Dry dynamics might also influence weakening or maintenance of MJO convection. Roundy (2022) showed that advection by upper tropospheric background wind substantially modulates the propagation speed of the MJO, with the slowest MJO events the most impacted. Roundy (2020) showed that, over the Indian Ocean, convectively coupled Kelvin waves and the MJO form a continuum, with upper tropospheric Kelvin wave structure dominant in intermediate disturbances and in the MJO itself. Kelvin wave-like features in the MJO include associated height anomalies in phase with zonal wind. The principal source of wind acceleration in a Kelvin wave and also in the equatorial upper tropospheric circulation signal of the MJO is the geopotential gradient force (Matsuno 1966, Sakaeda and Roundy 2015), but Kelvin waves are advected by and can advect the background flow as any other gravity wave. It is thus possible that interaction with the background wind may alter MJO propagation. Zhang and Han (2020) showed that MJO events are less likely to cross the Maritime Continent when the eastern Indian Ocean is anomalously cold and the western Pacific Ocean is anomalously warm. Their Figure 1c suggests that this pattern tends to co occur with lower tropospheric zonal mass confluence over the Maritime Continent. Lower tropospheric mass confluence tends to co occur with upper tropospheric mass diffluence. Upper tropospheric wind speeds are characteristically stronger, thus potentially yielding greater effects from dry dynamical processes such as advection of and by the background flow. This paper assesses the hypothesis that propagation of MJO upper tropospheric zonal wind across a region of background upper tropospheric zonal diffluence slows the MJO upper tropospheric circulation signal over the Indian Ocean and diminishes its amplitude over the Maritime Continent.

2. Data and Methods

MJO event days are identified over the eastern Indian Ocean during realtime multivariate MJO (RMM, Wheeler and Hendon 2004) index phase 3 with amplitude greater than one standard deviation. This choice of target phase places the MJO active convective signal just before it begins crossing the Maritime Continent. Data in this study are analyzed throughout the year to diagnose the signals associated with the full range of background winds (which vary with the seasonal cycle and other factors). Daily mean zonal wind u and geopotential gz data at 200 hPa on a 1° grid were obtained from the ERA5 reanalysis for 1979-2020 (Hersbach et al. 2023). Interpolated satellite outgoing longwave radiation (OLR) data on a 2.5-degree grid (Liebmann and Smith, 1996) were obtained from the NOAA Earth System Research Laboratory. The background zonal wind was calculated by applying an 80-day lowpass filter (via the Fourier transform) to the original u wind data. This 80-day boundary allows inclusion of background signals at periods just beyond the dominant timescale of the MJO. The primary and first 4 harmonics of the seasonal cycle were removed to create anomalies for the composite analysis. The zonal gradients of the geopotential anomaly, of the wind anomaly, and of the background zonal wind were obtained by using the centered finite difference in space (i.e., $\frac{\partial F}{\partial x} = \frac{F(x+1)-F(x-1)}{2\Delta x}$).

The negative zonal gradient of geopotential anomaly gives the geopotential gradient force, the principal source of acceleration of the winds in a Kelvin wave. The background gradient data were smoothed in the zonal direction with a 1-1-1 boxcar filter for plotting.

Advection of the background wind $\bar{u}$ by the anomalous wind u' is

$$adv_{\bar{u}} = -u'\frac{\partial \bar{u}}{\partial x}, \qquad (1)$$

And advection of the wind anomaly u' by the background wind is

$$adv_{u\prime} = -\bar{u}\frac{\partial u\prime}{\partial x}. \qquad (2)$$

An index of zonal diffluence over the Maritime Continent was created by averaging the first zonal finite difference of the 80-day low pass filtered zonal wind data over 90ºE to 120ºE (where the MJO signal has been observed to break down when it fails to cross the Maritime Continent). This index is standardized for reference by dividing by its standard deviation. Four composite events were made based on averaging the given data fields over the set of MJO event days meeting specified subsets of the RMM index phase 3 criteria. “All” events refers to the set of phase 3 event days not stratified by the Maritime Continent diffluence index. Confluent, diffluent, and neutral

MJO-day subsets refer to those RMM 3 days co occurring with negative (confluent) background zonal wind signal < –1 standard deviation, diffluent signal > +1 standard deviation, and neutral signal between –1 and +1 standard deviations. Statistical significance is assessed at the 99% confidence level by a 2-tailed students t-test assuming the null hypothesis that the true composite anomaly is zero.

3. Results

Figure 1 shows the Maritime Continent standardized zonal diffluence index of 200 hPa zonal wind between 90ºE and 120ºE. The signal historically varies between –3 and +3 standard deviations and shows substantial year to year variability. The blue curve includes seasonal variation while the green curve does not. The difference between them suggests a large seasonally evolving component. The blue curve is used for further analysis.

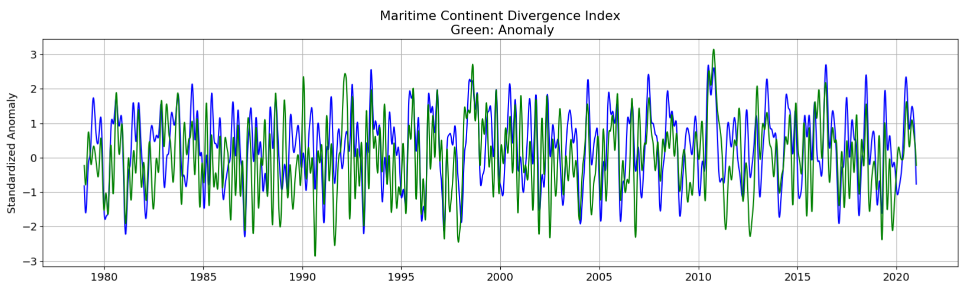

Figure 1: The blue curve is the Maritime Continent diffluence index averaged from 10ºN to 10ºS and from 90ºE to 120ºE, normalized by dividing by its standard deviation. The green curve is the anomaly from the seasonal cycle in the same quantity.

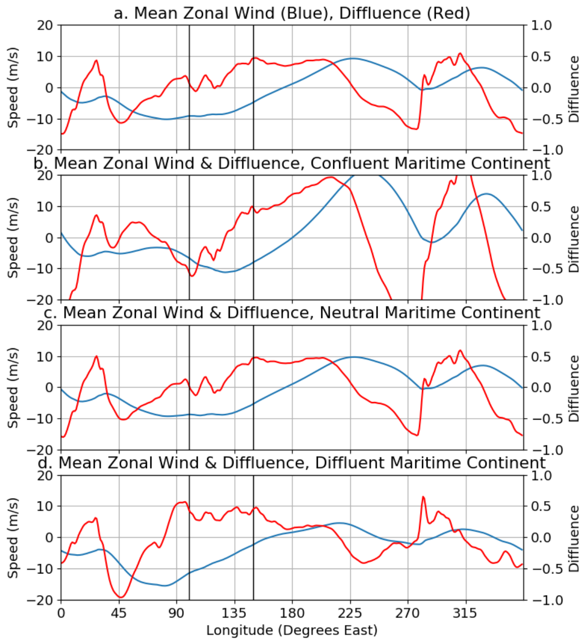

Figure 2: Time average zonal wind (blue) and zonal diffluence (red) as functions of longitude, averaged over times characterizing the different Maritime Continent average diffluence categories (a) the entire record, (b) confluent (diffluence < –1 Standard Deviation), (c) neutral (diffluence between + and –1 standard deviation), and (d) diffluent (diffluence > 1 standard deviation). Diffluence is scaled for plotting by a factor of 222,000m (twice the distance in meters between grid points). Vertical lines highlight the westernmost and easternmost extent of Maritime Continent Islands.

Figure 2 shows the mean state 10ºS to 10ºN 200 hPa equatorial zonal wind signal (blue curves), with easterlies dominating in the Eastern Hemisphere and Westerlies in the Western Hemisphere. The corresponding mean zonal diffluence is shown in red. Panel a represents the long-term mean, and panels b-d show confluent, neutral, and diffluent categories of the Maritime Continent diffluence index shown in Figure 1. In panel b, where diffluence is less than –1 standard deviation, the easterly wind over part of the Maritime Continent is the strongest in the world at the time, leading to upper tropospheric confluence (negative values in the red curve). In panel d, when 200 hPa diffluence over the Maritime Continent exceeds +1 standard deviation, the positive diffluence shown in the panel exceeds that observed during all the other shown subsets. A similar structure appears in the long-term average (panel a), suggesting stronger the contribution of diffluent periods to the long-term average. Panel d shows zonal wind over the Indian Ocean 4-5 ms^{-1} more easterly than the long-term average (panel a). The strongest amplitude structure in zonal wind and diffluence occurs in the Western Hemisphere, fluctuating wildly around South America, consistent with Sakaeda and Roundy (2015). The contrast between the region near and just east of 100ºE between panels b and d between the confluent and diffluent categories is the main focus difference of this project.

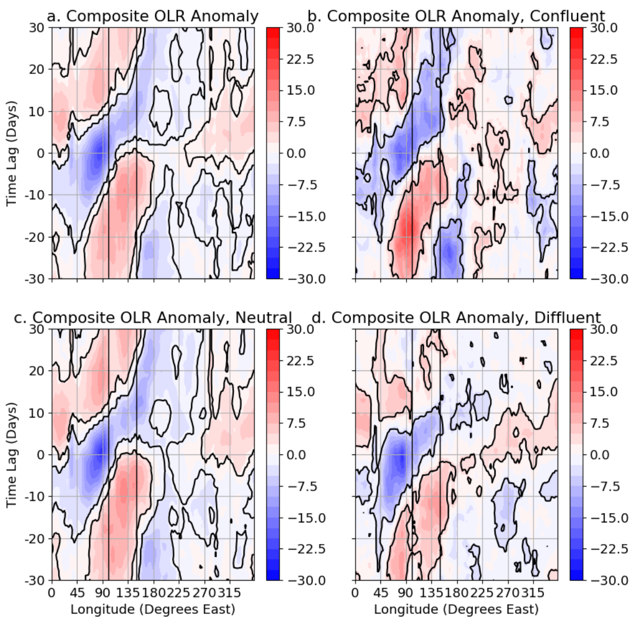

Figure 3: Composite RMM phase 3 events > amplitude 1 for (a) all events, (b), events in the Maritime Continent background confluent category, (c) events during neutral diffluence states, and (d) events during diffluent background conditions. Solid black contour indicates the 99% significance level by a student's t-test. Thin vertical lines darker than the grid highlight the location of the Maritime Continent.

Figure 3 shows lag composite OLR anomalies based on RMM phase 3 > amplitude 1.0 throughout the entire seasonal cycle. Black contours enclose regions that are statistically different from zero at above the 99% level. Consistent with each panel being in RMM 3 at lag = 0 days, convection near zero lag is present over the eastern Indian Ocean, moving slowly eastward (indicated by the blue-shaded region near the center-left of the composite). Convection begins in all panels prior to lag = –10 days over the western Indian basin. In all subgroups except the diffluent group (panel d), negative OLR anomalies cross the Maritime Continent (with substantial weakening in panels a and c), and then resume slow eastward propagation over the West Pacific Basin. One might argue that panel b shows a stalling signal over the Maritime Continent, but the location of the center of the negative OLR anomaly at 20-30 day lags is east of the central location at 0-10 day lags, and wind data discussed later demonstrate clear eastward propagation to the West Pacific Ocean. In the confluent group, panel b, negative OLR anomalies gain substantial amplitude over the west Pacific basin and then continue slowly eastward. In panel d, the negative OLR anomaly dramatically loses amplitude and breaks up as it crosses the Maritime Continent, with some suggestion of a weak and rapid eastward-moving signal over the Western Hemisphere. The slow eastward-propagation seen in panels a-c over the Maritime Continent and West Pacific regions is absent in panel d.

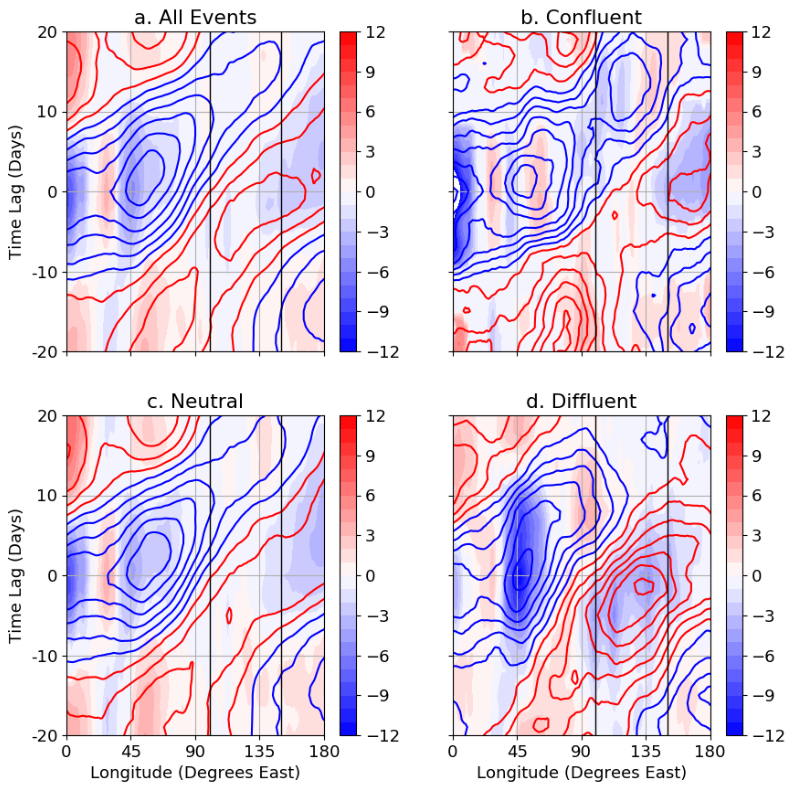

Figure 4: Composite 200 hPa zonal wind anomaly (contours, ms^{-1}) for RMM 3 for each of the 4 diffluence categories (a) All events, (b) confluent, (c) neutral, and (d) diffluent. Shading shows the advection of the background wind by the MJO composite zonal wind, scaled to ms^{-1} / 5 days. Positive (westerly) advection accelerations are red, shading levels are given every 1 ms^{-1} /5 days. Shaded regions not achieving statistical significance are set to zero. Vertical black lines outline the eastern and westernmost points of the Maritime Continent islands.

Figure 4 shows composite 200 hPa zonal wind anomaly (contours) and the corresponding accelerations (given in terms of ms^{-1} per 5 days) associated with advection of the background wind by the MJO-associated wind (shading). Panels a and c show easterly wind anomalies growing rapidly over the western Indian Ocean then gradually losing amplitude near the Maritime Continent, and then maintaining or slightly regrowing over the West Pacific region. The strongest easterly wind anomaly growth over the western Indian Ocean occurs together with easterly wind acceleration contributed by advection of the background wind by the MJO-associated wind in panel d. Panel b, for confluent conditions over the Maritime Continent, has fine structure alternating between easterly and westerly forcing by advection of the background wind over the western Indian Ocean, with less total acceleration of easterlies there by advection of the background wind than in the other panels. Although the panel b MJO easterly wind anomaly does not grow as rapidly over the western Indian Ocean, it maintains more amplitude over the Maritime Continent (focusing near 90-120ºE lag = 13 days), consistent with the easterly acceleration from the advected background wind along its trajectory there, which does not occur in the other three panels. The MJO easterly wind anomaly over the western Indian basin in panel d (near 45ºE lag = 0 days), in contrast, includes a strong surge of easterly momentum due to advection of like-signed background wind. Then the MJO easterly wind signal rapidly declines to near zero over the Maritime Continent as it mingles with westerly momentum from advection of the background wind (near 95ºE and lag = 5-15 days). The local amplification over the western Indian Ocean due to background confluence and collapse over the Maritime Continent associated with background diffluence are both consistent with a stronger Indian Basin Walker circulation associated with strong upper tropospheric easterly wind over the equatorial Indian Ocean (Fig. 2d). There is no statistically significant resurgence of MJO easterly wind along the slow path of West Pacific easterly wind anomalies present in the other panels. There is a weak and rapidly eastward moving easterly wind anomaly over the east Pacific Basin after lead = 10 days (not shown). A strongly fluctuating signal that occurs over the Western Hemisphere is not shown in Figure 4, to not complicate view of the focus regions over the warm pool. This fluctuating signal is especially strong during confluent Maritime Continent, when there is strong advection of the background wind by the MJO wind over the Western Hemisphere (see Figure 2), consistent with the earlier results of Sakaeda and Roundy (2015).

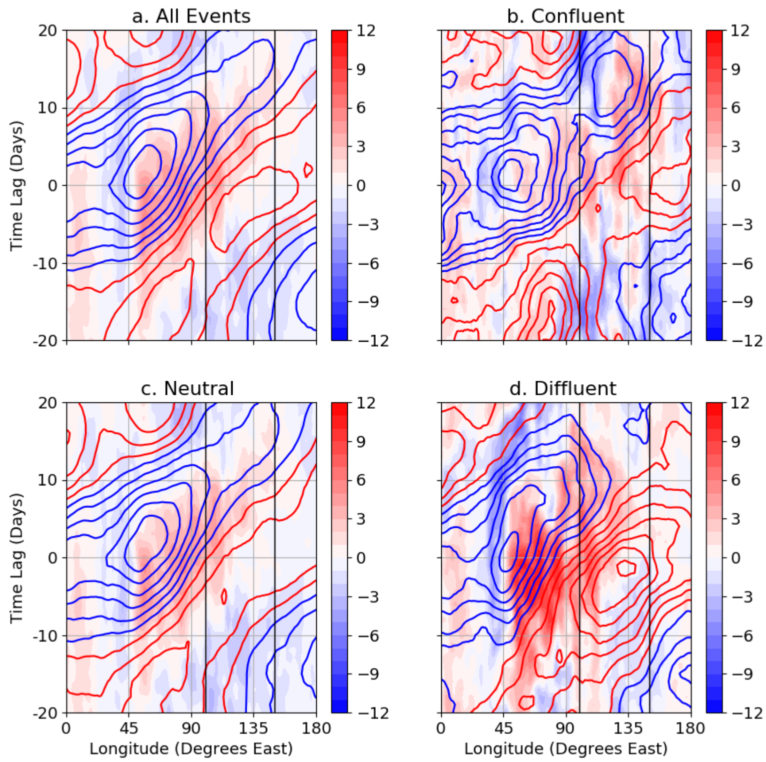

Figure 5: Composite zonal wind anomaly (ms^{-1}) and advection of the anomalous wind by the background wind $adv_{u'}$ as defined in equation (2) for the four diffluence conditions shown in Figures 3-4, (a) all events, (b) confluent conditions, (c) neutral, and (d) diffluent. Acceleration due to advection shown in the shading is represented as ms^{-1} per 5 days. The contour interval is every 2 ms^{-1}, with positive in red.

Figure 5 shows the advection of the anomalous zonal wind by the background wind as defined in equation (2). When averaged over the selected MJO event days, the result gives advection of the MJO-associated wind by the background wind. Panels a, c, and d show positive advection of the MJO wind to the east of the MJO easterly wind region centered near lag = 0 between 45ºE an d 90ºE. These accelerations in quadrature with MJO zonal wind anomalies reduce the eastward propagation speed of the MJO (Roundy 2022), and they substantially explain why the advancing MJO easterly wind signal slows down over the Western Indian Ocean. Positive advection in panel d is especially strong, exceeding 6 ms^{-1}/5 days, while associated negative accelerations are much less extensive along 45ºE and eastward over the Indian Ocean at leads of 0-20 days. The deceleration of the MJO by advection by the background wind is much less robust in confluent Maritime Continent conditions in panel b, where upper tropospheric easterly background wind is much weaker (Figure 2b).

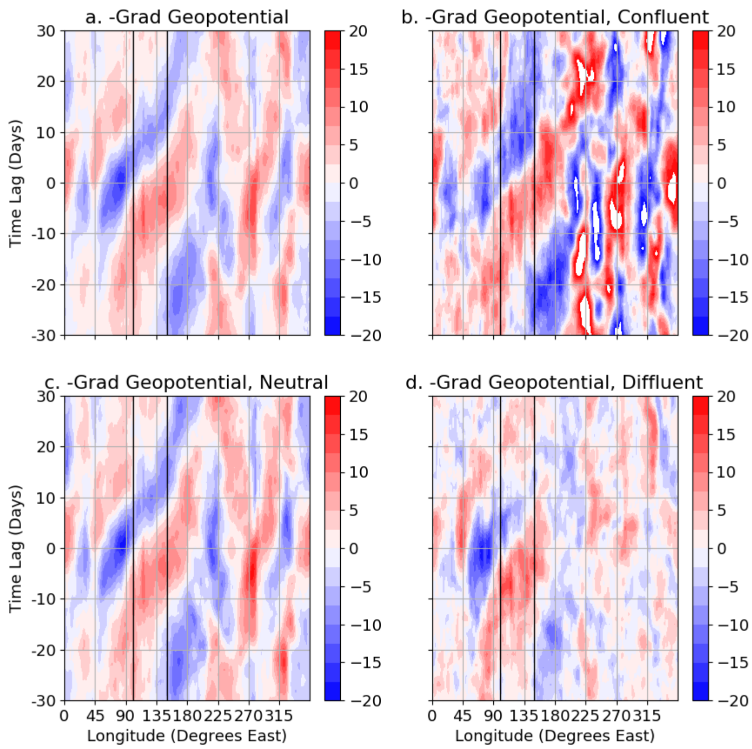

Figure 6: Composite $-\frac{dgz}{dx}$, the zonal geopotential gradient force, during each of the diffluence categories previously shown in Figures 3-5. Results are scaled to $ms^{-1}/5$ days.

Figure 6 shows the corresponding accelerations (scaled to $ms^{-1}/5$ days) in response to the geopotential gradient force corresponding to Figures 3-5 for the four Maritime Continent diffluence categories. This term is the leading acceleration term in Kelvin waves, and dominates the upper tropospheric zonal wind tendency in subseasonal variability in the equatorial warm pool region (Sakaeda and Roundy, 2015). The whole pattern is advected westward, or slowed down, over the warm pool by background easterly wind as shown by Roundy (2022) and Figure 5. The general pattern of amplification of the easterly wind accelerations over the western Indian Ocean is held in common with Figures 3-5, with some weakening in panels a and b over the Maritime Continent, while panels a through c show substantial and significant amplitude over the Western Pacific Ocean in the signal of acceleration of easterly wind shown in the blue shading. Panel b shows its strongest accelerations after day 10 near the Maritime Continent. In panel d, however, the acceleration of easterly wind damps to noise over the Maritime Continent, clearly showing the Maritime Continent barrier effect timed with when the upper tropospheric background zonal winds are most diffluent. The loss of OLR anomalies (Figure 3d), wind anomalies (Figure 4d), and geopotential gradient force anomalies (Figure 5d) suggest most of the MJO signal is damped out following RMM phase 3 events coinciding the diffluent upper tropospheric zonal wind over the Maritime Continent. At the same time, Figure 4d (red contours along the trajectory of MJO easterly wind) shows the direct contribution of the advection of the background wind to the decline of the MJO easterly wind anomaly, even as Figure 5d shows advection of the MJO-associated wind by the background flow strongly slowing the eastward propagation of the signal in this subset of events.

The correlations in time and longitude over the Indian Ocean and Maritime Continent region from 50ºE to 120ºE between the tendency of the composite zonal wind anomaly and each term considered here, $-\partial gz/\partial x$, $-u'\frac{\partial \bar{u}}{\partial x}$, and $= -\bar{u}\frac{\partial u'}{\partial x}$ for diffluent and confluent Maritime Continent are shown in Table 1. To focus on the dominant central signals in the composites, correlations are applied from time lags of –10 days to +15 days. To reduce redundant spatial signal, for significance testing, the domain was sampled every 5º of longitude instead of every degree. Results are not sensitive to these particular limits.

Table 1, Term Correlation Analysis against u Wind Tendency		
Diffluent Maritime Continent	Correlation	p-value
$-\partial gz/\partial x$	0.68	$2.6\text{x}10^{-50}$
$-\bar{u}\dfrac{\partial u'}{\partial x}$	–0.63	$2.0\text{x}10^{-42}$
$-u'\dfrac{\partial \bar{u}}{\partial x}$	0.05	0.38
Confluent Maritime Continent		
$-\partial gz/\partial x$	0.59	$2.4\text{x}10^{-35}$
$-\bar{u}\dfrac{\partial u'}{\partial x}$	–0.22	$2.0\text{x}10^{-10}$
$-u'\dfrac{\partial \bar{u}}{\partial x}$	–0.03	0.56

Table 1: Correlation analysis between the tendency of the composite 200 hPa zonal wind and the composites of the three terms examined here, for diffluent and confluent Maritime Continent, over 50ºE to 120ºE and time lags of –10 days to +15 days.

The factor among the 3 terms showing strongest correlation with the tendency of zonal wind is the geopotential gradient force, consistent with known dominance of Kelvin wave dynamics in the MJO equatorial upper tropospheric wind over the Indo Pacific warm pool (Sakaeda and Roundy 2015, Roundy 2020, 2021). Advection of the MJO wind by the background wind has statistically significant negative correlations with zonal wind tendency for both diffluent and confluent Maritime Continent, consistent with the conclusion that advection of the MJO wind by the background wind substantially slows the advance of the MJO zonal wind by offsetting the height gradient term. This signal is especially strong during diffluent Maritime Continent, consistent with the other results signaling the strong upper tropospheric background easterly wind over the Indian Ocean during diffluent Maritime Continent conditions (Figure 2d).

In neither diffluent nor confluent Maritime Continent is the advection of the background wind by the MJO wind significantly correlated with the tendency. This finding reflects not that this term is not physically relevant, but it instead reflects that this term is in phase with the MJO zonal wind rather than its tendency. The result is that it builds or deteriorates the wind anomaly in phase with the wind anomaly. The zero correlation between advection of the background wind by the MJO wind and tendency of the MJO wind emerges because its association with the tendency must reverse in time across a given wind anomaly. As an example, consider an MJO-associated easterly zonal wind anomaly crossing a region where the background wind is diffluent. At a given longitude, the MJO zonal wind tendency is negative prior to the maximum MJO easterly wind, then positive while the easterly wind anomaly declines. The contribution of advection of the background wind by the MJO wind must be positive, or westerly, across the whole MJO easterly wind anomaly, including both signs of its tendency. Therefore, an individual anomaly associated with this advection term must be uncorrelated with the MJO zonal wind tendency.

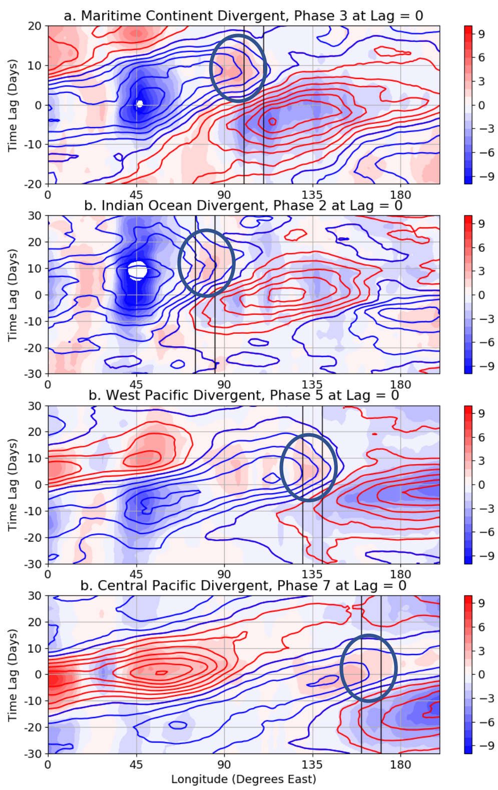

Figure 7: Content of Figure 4d repeated for MJO wind events during periods of diffluent background wind in the region between the two vertical lines on each panel. RMM phases for composites were selected to place the MJO easterly wind anomaly at lag = 0 just before arriving at the diffluent region between the vertical bars. Advection of the background wind by the MJO wind is shown in the shading, with westerly wind advection indicated in warm colors. Ellipses highlight regions of easterly wind anomaly decline intersecting the region of background diffluence.

These results raise the question whether advection of the background wind by the MJO wind has enhanced effect over the Maritime Continent due to other distinguishing characteristics of the region, or whether the associated barrier effect is driven mainly by more frequent and stronger diffluence signal at the Maritime Continent than other warm pool regions. To assess this concept I repeat the analysis for diffluent background zonal wind conditions at other locations across the warm pool. Figure 4d was replicated for different initial RMM states leading to MJO easterly wind anomalies approaching longitude regions over the Maritime Continent (as control, 100-110ºE, Panel a), eastern Indian Ocean (75-85ºE, Panel b), western Pacific Ocean (130-140ºE, Panel c), and central Pacific Ocean (160-170ºE, Panel d). A new index of diffluence of the background wind was calculated for each of these longitude regions to create composites. RMM phase at lag = 0 was assigned to 3 for Panel a, 2 for Panel b, 5 for Panel c, and 7 for panel d. Uniformly, in every panel, the MJO easterly wind anomaly collapses when it arrives at the region of upper tropospheric diffluence, and the decline coincides with advection of westerly background wind by the MJO wind (shading). This result suggests that the phenomenon of MJO collapse with this advection term is not unique to the Maritime Continent, but its common occurrence there would result from the region more frequently exhibiting stronger upper tropospheric zonal diffluence.

4. Conclusions

Figures 3-6 show that when the MJO active convective and upper tropospheric easterly wind anomalies located over the eastern Indian Ocean occur during periods of upper tropospheric diffluence of the background zonal wind over the Maritime Continent, the events subsequently tend to lose statistically significant amplitude in upper tropospheric zonal wind, geopotential height, and OLR anomalies, consistent with the Maritime Continent barrier effect. Results confirm the findings of Sakaeda and Roundy (2015), that the principal accelerations of the upper tropospheric zonal wind associated with the MJO over the Indian Ocean are driven by the geopotential gradient force, offset by advection of the MJO wind by the background easterly wind. The geopotential gradient force in a Kelvin wave propagates eastward in response to divergence of the eddy wind (Matsuno 1966). When background conditions are confluent over the Maritime Continent, zonal wind and the gradient of geopotential achieve greatest amplitudes over the Maritime Continent and the West Pacific basin. Figure 4 d shows that under conditions of background diffluence over the Maritime Continent, stronger than normal advection of upper tropospheric confluent background wind over the western Indian Ocean strengthens the upper tropospheric MJO zonal wind. The amplified MJO signal is then slowed in its eastward propagation as it is advected strongly westward by the enhanced upper tropospheric background easterly wind (Figure 5d). Then, as the MJO easterly wind anomaly moves eastward over the Maritime Continent, the MJO wind advects background wind of the opposite sign, counteracting its amplitude. The advection of the background wind by the MJO wind alters the amplitude of the MJO zonal wind anomalies by acting in line with the zonal wind, like the idealized event shown in Figure 8 (compare with Figure 4d).

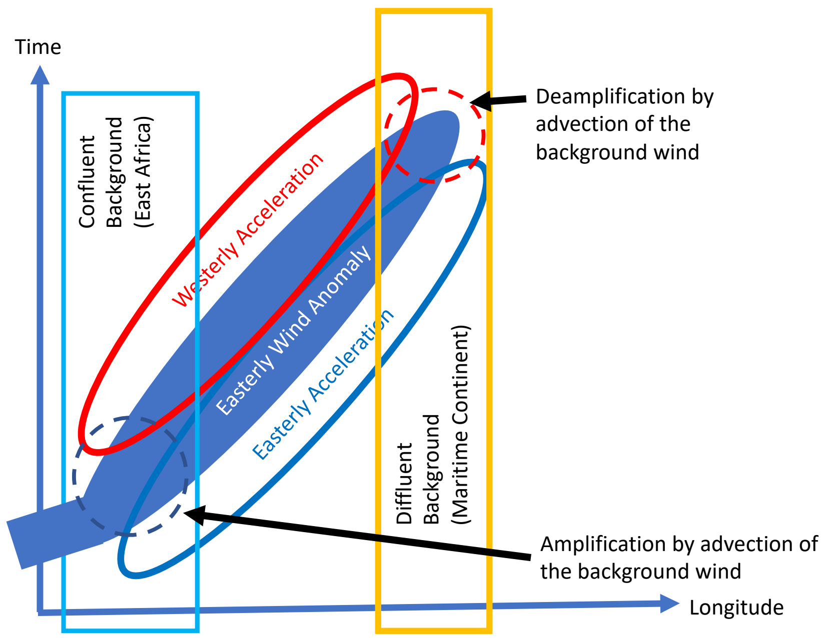

Figure 8: Schematic diagram of the longitude-time representation of an MJO upper tropospheric easterly wind anomaly during diffluent Maritime Continent. On arrival of the weak easterly wind anomaly from the west over East Africa, advection of easterly background wind grows the easterly wind anomaly. As it propagates eastward, it advances by easterly wind acceleration in quadrature with the easterly wind anomaly and declines by westerly wind acceleration, also in quadrature behind. Ultimately, the signal de amplifies to the east near the Maritime Continent as the easterly wind anomaly advects background wind of the opposite sign.

First, a weak MJO upper tropospheric easterly wind anomaly arrives from the west near East Africa (lower left of Fig. 8). There, advection of confluent background wind by the MJO wind amplifies the MJO easterly wind anomaly in phase with itself. As the easterly wind anomaly continues east across the Indian Ocean, acceleration of the wind is controlled by the sum of the geopotential gradient force and advection of the MJO wind by the background easterly wind (the total acceleration generated by these two terms is highlighted as easterly and westerly wind accelerations on Figure 8). On arrival at the Maritime Continent, advection of diffluent background wind by the MJO wind counteracts the MJO wind and the wind and convective signals then damp to zero. Since the resulting accelerations are in phase with the wind anomaly, zero correlation results between the zonal wind time tendency and advection of the background wind by the MJO wind, but it still yields a substantial weakening effect along the easterly wind anomaly trajectory. In events in which the MJO-associated zonal wind is diminished by superposition with wind of the opposite sign advected from the background wind, the weakened circulation must remove less mass east of the MJO-associated Kelvin wave trough, so the associated geopotential anomalies weaken as well (Figure 5d), which further damps the associated wind anomalies, and the whole signal collapses. The direct effects of convection are not considered here, but likely would result in reducing the amplitude of the MJO-associated upper tropospheric trough anomaly collocated with its easterly wind anomaly (because a convective mass source on the equator cannot create a trough above it and to its immediate west). This fact, the correlation analysis in Figure 1, and previous results of Sakaeda and Roundy (2015), Roundy (2020), and Roundy (2022) support the argument that the upper tropospheric equatorial zonal wind signal of the MJO over the Indian Ocean is fundamentally a planetary scale Kelvin wave altered by interaction with background flow.

The composite analysis was repeated for MJO events approaching regions of diffluence of the background wind at different locations across the warm pool, to assess whether the mechanism is unique to the Maritime Continent. Figure 7 shows that at each location, advection of background westerly wind by the MJO easterly wind coincides with dampening of the MJO easterly wind anomaly toward zero in the diffluent zone. Thus, this mechanism is not special to the Maritime Continent. However, since the Maritime Continent region is frequently diffluent, collapse of MJO events may occur there often.

Numerous authors have assessed sensitivity of the Maritime Continent barrier effect to various mechanisms, as discussed in the introduction. The mechanism discussed here does not necessarily exist in isolation from other mechanisms. Strong base state and diurnally varying convection over the Maritime Continent might compete with MJO convection crossing the region. Collapse of the upper tropospheric MJO circulation signal likely occurs at the same time that topography directly interferes with the lower tropospheric MJO convective signal. The region's background convection also associates with the strength of the Walker circulation and mass diffluence observed over the island region, so the various factors may be correlated. Nevertheless, direct computation of the advection terms shown here demonstrates their causal connection if not balanced by other factors, and balancing factors were not found in the broader project that included this analysis.

Numerical weather prediction models and global climate models on average show a stronger Maritime Continent barrier effect than observations. The findings herein suggest that these models might exhibit more consistently strong Maritime Continent convection and associated stronger upper tropospheric diffluence than in observations.

Acknowledgements

National Science Foundation grants 1757342 and 2103624 to Paul Roundy funded the related research. ERA5 reanalysis data was provided by ECMWF, and the NOAA ESRL provided OLR data.

Data Availability

ERA5 reanalysis data can be downloaded freely from ECMWF via the Copernicus website and OLR data from the NOAA ESRL. Code available from the author upon request (please give 2 weeks response time).

References

Abhik, S., H. H. Hendon, and C. Zhang, 2023: The Indo-Pacific Maritime Continent Barrier Effect on MJO Prediction. *J. Climate*, **36**, 945–957, https://doi.org/10.1175/JCLI-D-22-0010.1.

Ajayamohan, R. S., B. Khouider, V. Praveen, and A. J. Majda, 2021: Role of Diurnal Cycle in the Maritime Continent Barrier Effect on MJO Propagation in an AGCM. *J. Atmos. Sci.*, **78**, 1545–1565, https://doi.org/10.1175/JAS-D-20-0112.1.

Barrett, B.S., Densmore, C.R., Ray, P. *et al.* Active and weakening MJO events in the Maritime Continent. *Clim Dyn* **57**, 157–172 (2021). https://doi.org/10.1007/s00382-021-05699-8

Chen, G., J. Ling, C. Li, Y. Zhang, and C. Zhang, 2020: Barrier Effect of the Indo-Pacific Maritime Continent on MJO Propagation in Observations and CMIP5 Models. *J. Climate*, **33**, 5173–5193, https://doi.org/10.1175/JCLI-D-19-0771.1.

DeMott, C. A., Wolding, B. O., Maloney, E. D., & Randall, D. A. (2018). Atmospheric mechanisms for MJO decay over the Maritime Continent. *Journal of Geophysical Research: Atmospheres*, 123, 5188–5204. https://doi.org/10.1029/2017JD026979

Hendon, H. H., and M. L. Salby, 1994: The Life Cycle of the Madden–Julian Oscillation. *J. Atmos. Sci.*, **51**, 2225–2237, https://doi.org/10.1175/1520-0469(1994)051<2225:TLCOTM>2.0.CO;2.

Hersbach, H., Bell, B., Berrisford, P., Biavati, G., Horányi, A., Muñoz Sabater, J., Nicolas, J., Peubey, C., Radu, R., Rozum, I., Schepers, D., Simmons, A., Soci, C., Dee, D., Thépaut, J-N. (2023): ERA5 hourly data on pressure levels from 1940 to present. Copernicus Climate Change Service (C3S) Climate Data Store (CDS).

Hudson, J., and E. Maloney, 2023: The Role of Surface Fluxes in MJO Propagation through the Maritime Continent. *J. Climate*, **36**, 1633–1652, https://doi.org/10.1175/JCLI-D-22-0484.1.

Kim, D., Maloney, E. D., and Zhang, C., 2021: Review: MJO Propagation over the Maritime Continent. The Multiscale Global Monsoon System. Editor: Chih-Pei Chang. 261-272. https://doi.org/10.1142/11723

Liebmann, B, and C.A. Smith, 1996: Description of a Complete (Interpolated) Outgoing Longwave Radiation Dataset. *Bull. Amer. Meteorol. Soc.*, **77**, 1275-1277.

Ling, J., Zhang, C., Joyce, R., Xie, P.-p., & Chen, G. (2019). Possible role of the diurnal cycle in land convection in the barrier effect on the MJO by the Maritime Continent. *Geophysical Research Letters*, 46, 3001–3011. https://doi.org/10.1029/2019GL081962

Matsuno, T., 1966: Quasi-Geostrophic Motions in the Equatorial Area, *Journal of the Meteorological Society of Japan*. Ser. II, 44, 25-43.

Powell, S. W., and R. A. Houze, 2015: Effect of dry large-scale vertical motions on initial MJO convective onset. *J. Geophys. Res. Atmos.*, 120, 4783– 4805. doi: 10.1002/2014JD022961.

Roundy, P. E., and W. M. Frank, 2004: A Climatology of Waves in the Equatorial Region. *J. Atmos. Sci.*, **61**, 2105–2132.

Roundy, P. E., 2020: Interpretation of the spectrum of eastward-moving tropical convective anomalies. *Q J R Meteorol Soc*. 146: 795– 806. https://doi.org/10.1002/qj.3709

Roundy, P. E., 2022: Effect of Advection by Upper-Tropospheric Background Zonal Wind on MJO Phase Speed. *J. Atmos. Sci.*, **79**, 1859–1864, https://doi.org/10.1175/JAS-D-21-0298.1.

Sakaeda, N., and P. E. Roundy, 2015: The Development of Upper-Tropospheric Wind over the Western Hemisphere in Association with MJO Convective Initiation. *J. Atmos. Sci.*, **72**, 3138–3160, https://doi.org/10.1175/JAS-D-14-0293.1.

Wheeler, M. C., and H. H. Hendon, 2004: An All-Season Real-Time Multivariate MJO Index: Development of an Index for Monitoring and Prediction. *Mon. Wea. Rev.*, **132**, 1917–1932, https://doi.org/10.1175/1520-0493(2004)132<1917:AARMMI>2.0.CO;2.

Wheeler, M., & Kiladis, G. N. (1999). Convectively Coupled Equatorial Waves: Analysis of Clouds and Temperature in the Wavenumber–Frequency Domain, *Journal of the Atmospheric Sciences*, *56*(3), 374-399.

Zhang, C., and J. Ling, 2017: Barrier Effect of the Indo-Pacific Maritime Continent on the MJO: Perspectives from Tracking MJO Precipitation. *J. Climate*, **30**, 3439–3459, https://doi.org/10.1175/JCLI-D-16-0614.1.

Zhou, Y., S. Wang, J. Fang, and D. Yang, 2022: The Maritime Continent Barrier Effect on the MJO Teleconnections during the Boreal Winter Seasons in the Northern Hemisphere. *J. Climate*, **36**, 171–192, https://doi.org/10.1175/JCLI-D-21-0492.1.